Bulletin of Electrical Engineering and Informatics
Vol. 13, No. 3, June 2024, pp. 1638~1646
ISSN: 2302-9285, DOI: 10.11591/eei.v13i3.6836

Clutter evalution of unmanned surface vehicles for maritime traffic monitoring

Muhammad Nadiy Zaiaami[1], Nur Emileen Abd Rashid[2], Nor Najwa Ismail[3], Idnin Pasya Ibrahim[4], Siti Amalina Enche Ab Rahim[2], Nor Ayu Zalina Zakaria[1]
[1]School of Electrical Engineering, College of Engineering, Universiti Teknologi Mara, Selangor Malaysia
[2]Microwave Research Institute, Universiti Teknologi Mara, Selangor Malaysia
[3]NR Electrical and Electronic Enterprise, Selangor, Malaysia
[4]Department of Computer Science and Engineering, Division of Computer Engineering, University of Aizu, Aizuwakamatsu, Fukushima, Japan

Article Info

Article history:

Received May 30, 2023
Revised Dec 14, 2023
Accepted Dec 20, 2023

Keywords:

Distribution fitting
Goodness-of-fit
Maritime clutter
Maximum likelihood estimation
Root mean square error
Standard deviation

ABSTRACT

A traditional maritime radar system is utilized for ship detection and tracking through onshore transmitters and receivers. However, it faces challenges when it comes to detecting small boats. In contrast, unmanned surface vehicles (USVs) have been designed to monitor maritime traffic. They excel in detecting vessels of various sizes and enhance the capabilities and resolution of maritime radar systems. Nevertheless, just like conventional radar systems, USVs encounter difficulties due to environmental interference and clutter, affecting the accuracy of target signal detection. This research proposes a comprehensive numerical assessment to tackle the clutter issue associated with USVs. This involves gathering clutter signal data, performing numerical analysis, and employing distribution fitting techniques that leverage mathematical distributions to unravel data complexity. The root mean square error (RMSE) is applied in this analysis to validate the efficacy of the distribution model. The results of this study aim to formulate a clutter model that can enhance radar performance in detecting small vessels within cluttered environments.

Corresponding Author:

Nur Emileen Abd Rashid
Microwave Research Institute Universiti Teknologi Mara
40450 Shah Alam, Selangor, Malaysia
Email: emileen98@uitm.edu.my

1. INTRODUCTION

Conventional radar systems, which are responsible for transmitting and receiving signals, are typically placed on land to detect marine vessels [1]. The operation of this system consists of sending electromagnetic signals in the direction of the target and detecting and capturing those signals that are reflected back to the receiver. Not only does the signal that was received reveal the location of the target, but it also makes it possible to conduct an analysis of the target's size, direction, and velocity [2]. The conventional radar setup, on the other hand, frequently has a restricted number of degrees of freedom, which can be problematic when attempting to extract information from the station for use in remote sensing applications [3].

Maritime radar systems employ various frequencies, such as S-band, X-band, K-band, and C-band, to cater different requirements [4]. Extensive research substantiates that higher frequencies offer a more favorable prospect for detection [5]. By utilizing a 24 GHz frequency, superior detection resolution can be achieved, effectively mitigating false alarms. To circumvent delays associated with pulse waves, frequency

modulated continuous wave (FMCW) signals can be harnessed within radar systems. Numerous studies have successfully implemented a 24 GHz FMCW frequency in their investigations [6]. The utilization of K-band frequencies aids in minimizing detection errors [7]. Furthermore, the maritime radar community has employed a 24 GHz FMCW frequency for target detection and localization [8].

Figure 1 illustrates the propagation of an electromagnetic signal from the shoreline to a sea target (black dashed arrow), with subsequent reflection back to the receiver (red dashed arrow). The fidelity of the returned signal is compromised by unwanted reflections and refractions caused by factors like sea waves, atmospheric conditions, and avian disturbances known as "sea clutter" [9]. Previous works [3], [10], [11], focused on radar detection of large vessels such as ferries and cargo ships but challenges persist for smaller vessels like fisherman's boats. Researchers are now exploring unmanned surface vehicles (USVs) as a novel approach to improve resolution and capabilities of maritime radar systems [12].

Figure 1. Example of conventional radar

USVs, autonomous vehicles operating across terrains [13], are proven effective in surveillance and monitoring [14]–[16], widely used in civilian and military domains. In radar detection, bistatic radar implementation, eliminating bulky machinery [3], has promising results. The proposed approach involves leveraging USVs by equipping them with radar sensors and strategically deploying them at sea locations. However, sea clutter still affects detection probability, especially for small vessels.

Danklmayer *et al.* [17] introduces a novel sea-to-sea wave propagation method to mitigate sea clutter in maritime radar applications. This approach enhances sensing signals, improving radar cross section (RCS) returns for small boats through space diversity effects [18]. The study validates a newly developed clutter model through comprehensive numerical evaluation, aiming to improve existing radar systems and reduce clutter. However, literature on sea-to-sea wave propagation lacks numerical evaluation models for a comprehensive description of radar clutter in such systems.

Signal transmission from shore to sea creates triangulated reflections due to sea waves, resulting in disruptive sea clutter spikes [19]. To address this challenge, the study introduces a novel detection system utilizing a sensor mounted on a USV. The system gathers and analyzes data to investigate sea clutter characteristics, with a focus on sea-to-sea wave propagation and the utilization of space diversity.

The study aims to address adverse sea clutter effects on signal quality and enhance overall detection performance. This involves determining a suitable distribution that accurately represents clutter characteristics, utilizing a 24 GHz radar system for improved resolution and discrimination capabilities. The paper begins with a detailed explanation of radar requirements derived from a Fresnel zone study, followed by an examination of experimental configuration and numerical analysis of clutter phenomena. The study includes a comprehensive analysis of the distribution model. The final section outlines future work for advancing a maritime clutter model tailored for USVs. Experimental results can improve radar system performance for small vessel detection and weather forecasting through numerical evaluation and data fitting [20]–[22].

2. METHODOLOGY

The comprehensive study as depicted in Figure 2, begins with the determination of the important radar requirements for the placement and configuration of the transceiver. This is achieved by utilizing the concept of the Fresnel zone. Following this, the experimental configuration is customized to align with the capabilities of the *Pusat Penyelidikan Air Malaysia* (NAHRIM) facility, facilitating the production of artificial sea waves with predetermined heights and intervals. After a collection of cluttered data, the Hilbert transform is utilized to extract the amplitude, thereby improving the quality of the data. The processed data is utilized to reveal the hidden Doppler information signal. By employing the parameters obtained from the analysis above, a thorough

evaluation of clutter measurement is conducted by constructing probability distribution functions (PDFs) that encompass log-normal, log-logistic, gamma, and weibull distributions. In this study, various quantitative metrics are employed to evaluate the distributions under investigation. These metrics include maximum likelihood estimation (MLE), standard deviation (STD), goodness-of-fit (GOF), and root mean square error (RMSE). The computed values of these metrics for each distribution are then presented and discussed in the subsequent results section.

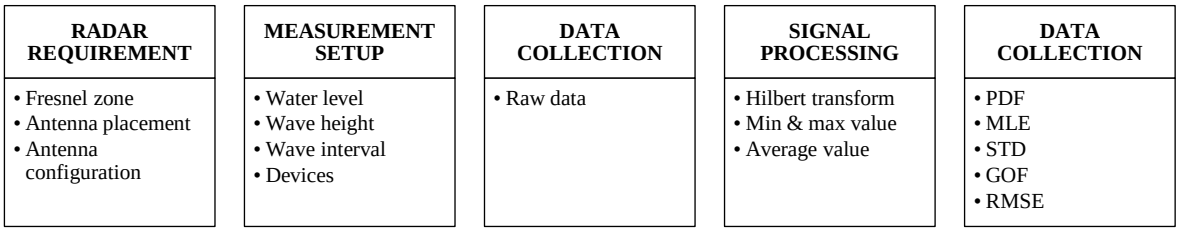

Figure 2. Clutter evaluation process flow

2.1. Radar requirement estimation

Mounting the transceiver in radar requirement estimation involves considering the Fresnel zone for optimal signal propagation, crucial for detecting surrounding objects and minimizing blind spots. A comprehensive monitoring system allows a 360-degree view of the radar's surroundings [23]. The height of the radar system's antenna directly affects transmitting and receiving antenna angles, as extensively studied at a 5 GHz frequency [4]. These investigations offer valuable insights into radar system design, ensuring optimal functionality and performance [24].

Depending on the size of the USV, placing transmitting and receiving antennas at a height of 1 m above the ground is sufficient to eliminate destructive ground waves that could interfere with the radar processing. Figure 3 is the illustration of the concentric ellipse of transmission of the antenna. The total distance from the transmitting and receiving antenna is 10 m which d_1 and d_2 are both 5 m while h_t and h_r are both 1 m. The Fresnel zone can be calculated by using the basic (2):

$$Radius\ (mts.) = 17.31 \times \sqrt{\frac{D\ (in\ km)}{4 \times f\ (in\ GHz)}} \tag{1}$$

where D is the distance of the transmitting antenna to the center of the transmission path, and r is the radius of the concentric ellipse respectively as shown in Figure 3.

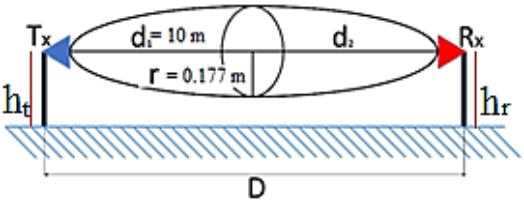

Figure 3. Concentric ellipse of transmission

Utilizing a distance, D of 10 m and an operating frequency of 24 GHz, the radius, r of the Fresnel zone can be determined where the calculated radius is found to be 0.177 m. Notably, this value represents the minimum height requirement for the antenna to prevent ground reflections and maintain optimal performance. Failure to adhere to this minimum antenna height would result in undesired beamwidth bouncing off the ground, leading to undesirable ground reflections and subsequent impact on the radar system's overall performance. Therefore, ensuring a minimum antenna height of 0.177 m is essential to mitigate these adverse effects and maintain the desired operational characteristics of the radar system. This calculation and requirement contribute to the accurate design and implementation of radar systems, optimizing their performance in practical applications. The height of antenna placement in this study is placed 1 and 1.5 m above sea water level which exceeds the minimum height of antenna placement as per calculated above.

2.2. Measurement setup

Data collection and clutter measurement for this study take place at NAHRIM, a renowned research institution with expertise in water-related investigations. To ensure accuracy, experimental parameters are carefully set and maintained in a controlled environment. Due to limitations in wave height at NAHRIM, a 1:100 scale-down approach is employed, allowing for accurate representation of real-world conditions while facilitating precise measurements and data collection.

The experiment is conducted in a basin of 30 m^2. An artificial sea wave is generated by using a wave generator at the end of the basin and the transceiver is mounted facing toward the wave generator as shown in Figure 4(a). During the measurement, an OmniPreSense radar sensor is used to collect the clutter signals where the wave signal is propagated on the water surface, bounced back, and received by the receiver antenna. Each data is collected for 60 s and the total of data collected for this analysis is 30 data. The collected signal includes noise and clutter along the parameter. It is initially processed to determine the average values, which are then subtracted from the raw data to obtain the mean value. Subsequently, the processed data underwent a Hilbert transformation to extract the amplitude of the clutter. The resulting processed data, characterized by its enhanced signal quality, will be utilized to determine the enveloped signal of the Doppler information.

Figure 4(b) presents a side view of an illustrative depiction of a transceiver system positioned above the water surface, highlighting the key elements and processes involved in sea-to-sea wave propagation. The transceiver antenna, denoted as TX (transmitter) and RX (receiver), serves as the source and destination for signal transmission, respectively. Upon transmission from the transceiver antenna, the electromagnetic signal propagates across the water surface, exhibiting a characteristic bouncing effect, before ultimately returning to the transceiver antenna. This phenomenon, known as sea-to-sea wave propagation, plays a pivotal role in the formation and behavior of the transmitted signal. Notably, the height of the transceiver antenna is represented as h, while Iw and hw symbolize the wave interval and wave height, respectively. The blue and red arrows in Figure 4 visually represent the propagation of the signal along the water's surface. A comprehensive understanding of these parameters and the underlying sea-to-sea wave propagation mechanisms is crucial for accurately assessing the impact of sea clutter on signal quality and devising effective mitigation strategies. The transceiver configuration during data collection is shown in Figure 5 where the antenna is securely mounted on a pole positioned above the seawater surface before the wave is generated, while the parameters used are tabulated in Table 1.

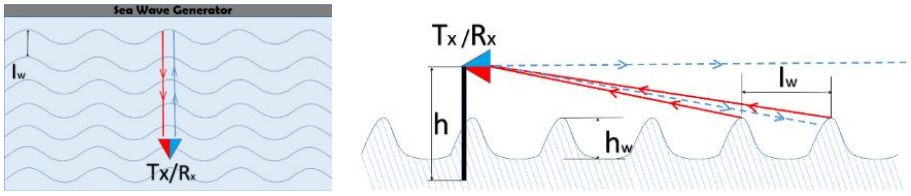

(a) (b)

Figure 4. Illustration of antenna placement; (a) top view and (b) side view

Figure 5. Actual transceiver configuration

Table 1. Measurement parameters and value

Parameters	Value
Antenna height (*h*)	1 and 1.5 m
Antenna configuration	Transceiver
Wave height (*hw*)	10 and 20 cm
Wave interval (*Iw*)	2s

2.3. Numerical analysis of clutter data

This section delves into the mathematical models utilized to represent distinct clutter signal samples. The determination of parameters for each model is based on mathematical equations specifically tailored for this purpose. The core objective of this analysis is to ascertain the parameter values of the optimal-fit distribution model by leveraging the measured clutter data. The primary focus of this analysis centers around the PDF of Weibull, Gamma, log-logistic, and log-normal distributions as summarized in Table 2, which have garnered considerable interest despite the presence of several alternative models in the existing literature.

Table 2. Distribution model

No.	Distributions	Description	Mathematical format
1	Log-normal distribution	The log-normal distribution, defined by μ and σ, models positive data by exponentiating a normally distributed random variable, with μ as the location and σ as the scale.	$(f(x\|\mu,\sigma) = \frac{1}{x\sigma\sqrt{2\pi}}\ exp\left\{\frac{-(\ln x-\mu)^2}{2\sigma^2}\right\};\ x \geq 0$
2	Log-logistic distribution	The log-logistic distribution, similar to the log-normal distribution, features heavier tails. It is often employed in survival analysis for parametric modeling of events with increasing and decreasing rates.	$(f(x\|\mu,\sigma) = \frac{1}{\sigma}\frac{1}{x}\frac{e^z}{(1+e^z)^2}\ ;\ x \geq 0$ where $z = \frac{\log(x)-\mu}{\sigma}$
3	Gamma distribution	The Gamma distribution model is a continuous distribution where it is the sum of exponentially distributed random variables.	$(f(x\|a,b) = \frac{1}{b^a\Gamma(a)}x^{a-1}e^{\frac{-x}{b}}$
4	Weibull distribution	Is a continuous probability distribution using positive only values of data. Strictly positive values of the shape parameter *b* and scale parameter *a*.	$(f(x\|a,b) = \frac{b}{a}(\frac{x}{a})^{b-1}e^{-(\frac{x}{a})^b}$

The numerical evaluation of the clutter data will go through all these distributions and calculations such as MLE, STD, GOF, and RMSE are made for each distribution model. To identify and validate the model that exhibits the least error between the clutter data and the statistical model, a GOF test approach employing the RMSE method is employed in this analysis.

MLE is utilized to determine the parameters of fitting for each distribution. The parameters include the values of *(μ)* and *(σ)*, which are used with the log-normal and log-logistic distributions. In contrast, alpha *(α)* and *(β)* values are determined for the Gamma and Weibull distributions. STD is the square root of the variance data sample to determine an error for each distribution parameter, as shown in (2), where μ for population data and σ is sample data.

$$\sigma = \sqrt{\frac{1}{N}\sum_{i=1}^{n}(x_i - \mu)^2} \quad (2)$$

The GOF for the statistical models is evaluated using the RMSE method [25]. RMSE, defined as the standard deviation of the residuals or prediction errors, serves as a measure of the accuracy of the fitted distributions. The distribution that exhibits the lowest percentage error is considered the most suitable fit. To assess the GOF, RMSE is calculated for each distribution by comparing the amplitude values of the sample clutter data (c_i) with the corresponding amplitude values of the statistical model ($\hat{c}_i$). The RMSE value is computed using (3), where *i* represents the sample clutter data number. This rigorous evaluation contributes to the assessment of the GOF and enhances the reliability of the statistical modeling process.

$$\text{RMSE}=\sqrt{\frac{1}{n}\sum_{i=1}^{n}(c_i - \hat{c}_i)^2} \quad (3)$$

3. RESULTS AND DISCUSSION

The findings of this analysis have been divided into two sections: clutter processing and numerical analysis of a clutter signal that represents a distinct wave height corresponding to a specific antenna height. For numerical analysis, the following distribution models are chosen for each category of wave height: Weibull, Gamma, log-logistic, and log-normal. Table 3 contains tabular representations of the calculated parameters, STD, and RMSE values for all models, respectively.

Table 3. Distribution model parameters, STD, and percentage of RMSE

Parameters		STD and STD Err	PDF			
			Log-logistic	Log-normal	Gamma	Weibull
1 m antenna	10 cm wave height	STD	μ=2.0723	μ=1.9872	a=2.9006	a=9.8326
		6.8810	σ=0.3574	σ=0.7226	β=3.0176	β=2.0157
		STD Err	$RMSE_{LL}$=0.0034	$RMSE_{LN}$=0.0040	$RMSE_G$=0.0033	$RMSE_W$=0.0030
		0.0089	%err.=0.3426	%err . =0.4024	%err . =0.3318	%err . =0.3010
	20 cm wave height	STD	μ=2.1191	μ=2.0377	a=3.1806	a=10.1741
		6.4416	σ=0.3336	σ=0.6838	β=2.8461	β=2.0916
		STD Err	$RMSE_{LL}$=0.0044	$RMSE_{LN}$=0.0052	$RMSE_G$=0.0044	$RMSE_W$=0.0040
		0.0083	%err . =0.4352	%err . =0.5160	%err . =0.4364	%err . =0.3997
1.5 m antenna	10 cm wave height	STD	μ=2.4030	μ=2.3507	a=4.1578	a=13.4062
		8.3440	σ=0.2942	σ=0.5513	β=2.8598	β=2.3662
		STD Err	$RMSE_{LL}$=0.0034	$RMSE_{LN}$=0.0037	$RMSE_G$=0.0033	$RMSE_W$=0.0031
		0.0108	%err .=0.3393	%err .=0.3682	%err .=0.3277	%err .=0.3108
	20 cm wave height	STD	μ=2.1583	μ=2.0813	a=2.6761	a=10.9842
		8.1620	σ=0.3813	σ=0.7285	β=3.6520	β=1.8715
		STD Err	$RMSE_{LL}$=0.0033	$RMSE_{LN}$=0.0036	$RMSE_G$=0.0030	$RMSE_W$=0.0027
		0.0106	%err .=0.3294	%err .=0.3637	%err .=0.2958	%err .=0.2681

3.1. Clutter processing

As mentioned earlier, a comparative analysis is conducted in the time domain to evaluate the processed data obtained from antennas positioned at heights of 1 and 1.5 m. Throughout the experiments, the wave height is kept constant (either 10 cm or 20 cm) while the antenna heights are varied. The processed time domain clutter signal, focusing on the initial 60 s, is displayed in Figures 6(a) and (b) for antenna heights of 1 m and 1.5 m, respectively, while considering a wave height of 10 cm. In Figure 6(a), corresponding to the 1 m antenna height, the amplitude clutter signal is observed to range from 12 to 30, with an average amplitude value of 18. Conversely, Figure 6(b) portrays the clutter signal for the 1.5 m antenna height, exhibiting an amplitude range of 22 to 38, and an average amplitude value of 27.

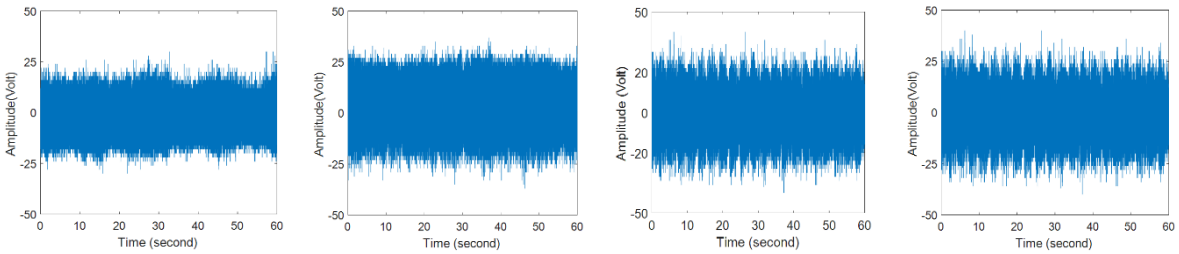

Figure 6. Time domain clutter signal for with 1 m and 1.5 m antenna height; (a) 10 cm wave height and (b) 20 cm wave height

Further investigation is conducted to examine the impact of a higher wave height, specifically set at 20 cm. Figure 6 illustrates the time domain clutter signal obtained under two different antenna heights, namely 1 m (Figure 6(a)) and 1.5 m (Figure 6(b)). In the case of an antenna height of 1 m, the range of the amplitude clutter signal, as depicted in Figure 6(a), varied from 17 to 40. Notably, the average value of the amplitude signal is measured to be 22. On the other hand, when the antenna height is increased to 1.5 m, the range of the amplitude clutter signal exhibited a slightly different pattern, ranging from 15 to 40. Remarkably, the average value of the amplitude signal in this scenario is recorded as 24, as illustrated in Figure 6(b). This analysis provides valuable insights into the influence of wave height and antenna height on the characteristics of the clutter signal, contributing to a deeper understanding of radar system performance.

Figure 7(a) depicts the amplitude-enveloped signal for 20 cm wave heights, which exhibits significantly larger magnitudes than the signal for 10 cm wave heights. This variation in amplitude can be attributed to the spatial limitations imposed by lower antenna heights, which result in reduced surface coverage. Despite these limitations, it is notable that the radar system collects a greater amount of clutter in the case of higher wave heights (20 cm versus 10 cm). This finding highlights the impact of varying sea wave heights on system noise, indicating that higher waves generate more significant interference in radar clutter. Meanwhile, Figure 7(b) depicts a comparison of the enveloped signals of 10 cm and 20 cm wave heights for a fixed 1.5 m antenna, revealing that the amplitudes for each wave height are only slightly different. The amplitude of interference is not overly significant since larger antennas cover a larger area and therefore capture more interference into the system.

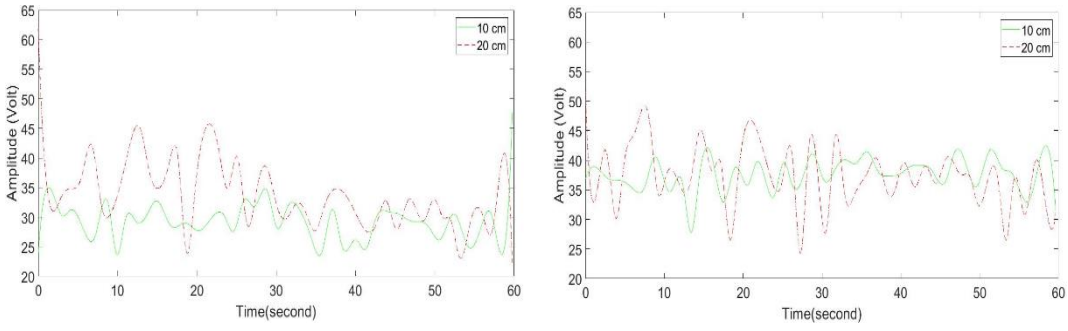

Figure 7. Envelope signal; (a) 1 m antenna height and (b) 1.5 m antenna height

3.2. Distribution fitting and numerical analysis of clutter data

Figure 8 presents a comprehensive analysis of the clutter signal probability plot, showcasing a comparison of four fitting models: log-normal, log-logistic, Gamma, and Weibull distributions. The probability plots are displayed for both a wave height of 10 cm and 20 cm, considering antenna heights of 1 m and 1.5 m. In Figure 8(a), the probability plot for the clutter signal with a 10 cm wave height is depicted for antenna heights of 1 and 1.5 m, respectively. Additionally, Figure 8(b) represents the probability plot for the clutter signal with a wave height of 20 cm, again for antenna heights of 1 and 1.5 m.

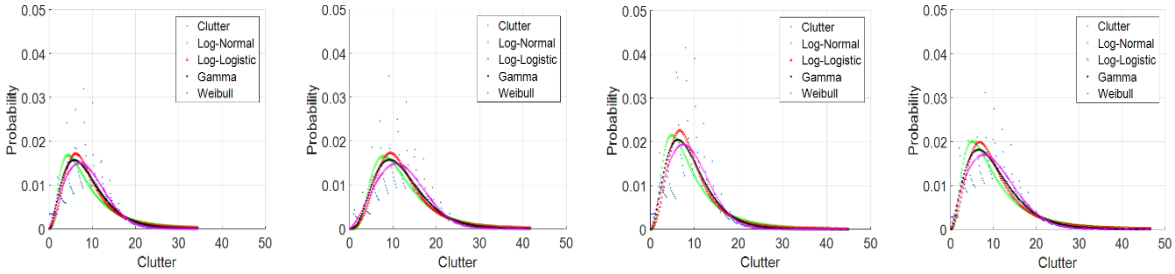

Figure 8. Distribution fitting for with 1 m and 1.5 m antenna height; (a) 10 cm wave height and (b) 20 cm wave height

Remarkably, the Weibull distribution emerged as the most suitable fitting model across all probability plots. This implies that the Weibull distribution effectively captures the statistical characteristics of the clutter signal. Furthermore, it is noteworthy that the probability plots exhibit greater scatter for the higher wave height scenario. This observation can be attributed to the increased clutter signal generated by higher wave heights, which consequently exerts a significant impact on radar system performance. These findings provide valuable insights into the selection of appropriate distribution models and the understanding of radar performance in the presence of varying wave heights.

4. CONCLUSION

Radar-based USVs can overcome the limitations of conventional maritime radar in detecting small vessels. However, it still suffers from the effect of clutter, which can reduce the probability of detection; this can be resolved by analyzing the optimal distribution and comprehending the characteristics of clutter. The Weibull distribution is the best-fitting distribution in this investigation, based on the preceding finding. This is confirmed by the RMSE value, which provides the lowest error rate, and this evaluation promises a higher resolution for vessel detection in maritime radar. These results also demonstrate a significant differential effect, suggesting that antenna placement at a higher altitude above sea level results in increased surface coverage. However, it captures a greater amount of noise and interference from the environment. As a result, it is crucial to take antenna height into account when designing and deploying radar systems, as it has a direct impact on the characteristics of clutter and the overall efficacy of the radar system. This finding will contribute to the modeling of maritime USV clutter, which can be used to reduce false alarms and enhance the detection resolution of small vessels.

ACKNOWLEDGEMENTS

This research was financially supported by Universiti Teknologi MARA and Microwave Research Institute.

REFERENCES

[1] F. S. de Adana, "The first maritime navigation radars in spain after the second world war [historical corner]," *IEEE Antennas and Propagation Magazine*, vol. 57, no. 5, pp. 152–158, Oct. 2015, doi: 10.1109/MAP.2015.2471999.

[2] M. Kirscht *et al.*, "An airborne radar sensor for maritime and ground surveillance and reconnaissance-algorithmic issues and exemplary results," *IEEE Journal of Selected Topics in Applied Earth Observations and Remote Sensing*, vol. 9, no. 3, pp. 971–979, Mar. 2016, doi: 10.1109/JSTARS.2015.2418173.

[3] H. Griffiths, "Developments in bistatic and networked radar," in *Proceedings of 2011 IEEE CIE International Conference on Radar*, pp. 10–13, Oct. 2011, doi: 10.1109/CIE-Radar.2011.6159708.

[4] J. Stepien, "Review of S-band and X-band antennas and filters for both maritime and space applications," in *2020 International Symposium on Antennas and Propagation (ISAP)*, pp. 783–784, Jan. 2021, doi: 10.23919/ISAP47053.2021.9391465.
[5] I. Gresham *et al.*, "Ultra-wideband radar sensors for short-range vehicular applications," *IEEE Transactions on Microwave Theory and Techniques*, vol. 52, no. 9, pp. 2105–2122, Sep. 2004, doi: 10.1109/TMTT.2004.834185.
[6] G. Gennarelli, C. Noviello, G. Ludeno, G. Esposito, F. Soldovieri, and I. Catapano, "24 GHz FMCW MIMO radar for marine target localization: a feasibility study," *IEEE Access*, vol. 10, pp. 68240–68256, 2022, doi: 10.1109/ACCESS.2022.3186052.
[7] Y. Kong and N. Yan, "High gain and low flicker noise down-conversion mixer applied in 24GHz FMCW radar," in *2018 IEEE MTT-S International Wireless Symposium (IWS)*, pp. 1–4, May 2018, doi: 10.1109/IEEE-IWS.2018.8400984.
[8] H. Zhang, L. Li, and K. Wu, "24GHz software-defined radar system for automotive applications," in *2007 European Conference on Wireless Technologies*, pp. 138–141, Oct. 2007, doi: 10.1109/ECWT.2007.4403965.
[9] F. Sermi, C. Mugnai, F. Cuccoli, and L. Facheris, "A maritime radar network for surface traffic control based on service vessels," in *Proceedings International Radar Symposium*, vol. 1, pp. 252–257, 2013.
[10] K. Laws, J. Vesecky, and J. Paduan, "Monitoring coastal vessels for environmental applications: Application of Kalman filtering," in *2011 IEEE/OES 10th Current, Waves and Turbulence Measurements (CWTM)*, pp. 39–46, Mar. 2011, doi: 10.1109/CWTM.2011.5759521.
[11] J. Carretero-Moya, A. De Maio, J. Gismero-Menoyo, and A. Asensio-Lopez, "Experimental performance analysis of distributed target coherent radar detectors," *IEEE Transactions on Aerospace and Electronic Systems*, vol. 48, no. 3, pp. 2216–2238, Jul. 2012, doi: 10.1109/TAES.2012.6237589.
[12] K. R. Bennett, J. Zeng, D. Diggins, L. Nonas-Hunter, C. Snow, and A. A. Bennett, "The development and implementation of an automated coastal environment monitoring system," in *Global Oceans 2020: Singapore–U.S. Gulf Coast*, pp. 1–5, Oct. 2020, doi: 10.1109/IEEECONF38699.2020.9389011.
[13] A. Romano and P. Duranti, "Autonomous unmanned surface vessels for hydrographic measurement and environmental monitoring," *FIG Working Week*, no. pp. 1–15, May 2012, 2012.
[14] A. Stateczny, W. Kazimierski, P. Burdziakowski, W. Motyl, and M. Wisniewska, "Shore construction detection by automotive radar for the needs of autonomous surface vehicle navigation," *ISPRS International Journal of Geo-Information*, vol. 8, no. 2, Feb. 2019, doi: 10.3390/ijgi8020080.
[15] Z. Liu, Y. Zhang, X. Yu, and C. Yuan, "Unmanned surface vehicles: An overview of developments and challenges," *Annual Reviews in Control*, vol. 41, pp. 71–93, 2016, doi: 10.1016/j.arcontrol.2016.04.018.
[16] C. Almeida *et al.*, "Radar based collision detection developments on USV ROAZ II," in *OCEANS 2009-EUROPE*, pp. 1–6, May 2009, doi: 10.1109/OCEANSE.2009.5278238.
[17] A. Danklmayer, T. Brehm, G. Biegel, and J. Forster, "Multi-frequency propagation measurements over a horizontal path above the sea surface in the Baltic Sea," in *2013 7th European Conference on Antennas and Propagation, EuCAP 2013*, pp. 2526–2527, 2013.
[18] I. Pasya, N. Iwakiri, and T. Kobayashi, "Performance of joint direction-of-departure and direction-of-arrival estimation in UWB MIMO radars detecting targets with fluctuating radar cross sections," in *2014 11th European Radar Conference*, pp. 277–280, Oct. 2014, doi: 10.1109/EuRAD.2014.6991261.
[19] F. L. Posner, "Spiky sea clutter at high range resolutions and very low grazing angles," *IEEE Transactions on Aerospace and Electronic Systems*, vol. 38, no. 1, pp. 58–73, 2002, doi: 10.1109/7.993229.
[20] Y. Wei, L. Guo, and J. Li, "Numerical simulation and analysis of the spiky sea clutter from the sea surface with breaking waves," *IEEE Transactions on Antennas and Propagation*, vol. 63, no. 11, pp. 4983–4994, Nov. 2015, doi: 10.1109/TAP.2015.2476375.
[21] V. T. Vakily and M. Vahedi, "Sea clutter modeling improvement and target detection by tsallis distribution," in *2009 International Conference on Advanced Computer Control*, pp. 715–719, 2009, doi: 10.1109/ICACC.2009.90.
[22] J. Hu, W. Tung, and J. Gao, "Modeling sea clutter as a nonstationary and nonextensive random process," in *2006 IEEE Conference on Radar*, pp. 412–416, doi: 10.1109/RADAR.2006.1631833.
[23] S. Kaul *et al.*, "Effect of antenna placement and diversity on vehicular network communications," in *2007 4th Annual IEEE Communications Society Conference on Sensor, Mesh and Ad Hoc Communications and Networks*, pp. 112–121, Jun. 2007, doi: 10.1109/SAHCN.2007.4292823.
[24] J. Howell, "Microstrip antennas," in *1972 Antennas and Propagation Society International Symposium*, vol. 10, pp. 177–180, 1972, doi: 10.1109/APS.1972.1146932.
[25] P. Li, J. Xie, and B. Zhang, "Modelling of sea clutter with generalized exponential distribution," in *2020 IEEE 5th International Conference on Signal and Image Processing (ICSIP)*, pp. 562–566, Oct. 2020, doi: 10.1109/ICSIP49896.2020.9339276.

BIOGRAPHIES OF AUTHORS

Muhammad Nadiy Zaiaami received the Bachelor Engineering Technology in Electrical from University Kuala Lumpur (UniKL) in 2012 and M.Sc. in Telecommunication and Information Engineering in from Universiti Teknologi MARA (UiTM) in 2016. He is currently pursuing his study in Ph.D. (Electrical Engineering) at UiTM in modelling clutter distribution. He can be contacted at email: nadiyzaiaami@gmail.com.

Nur Emileen Abd Rashid completed her Bachelor of Engineering in Electrical Engineering (Communications) at Universiti Kebangsaan Malaysia (UKM). She successfully earned her Ph.D. in Electrical Engineering with a specialization in Radar Technology from the University of Birmingham, UK. Currently, she serves as a research fellow at Microwave Research Institute, UiTM. She can be contacted at email: emileen98@uitm.edu.my.

Nor Najwa Ismail received a Bachelor of Engineering (Hons) in Electronics (Communication) from the Faculty of Electrical Engineering, Universiti Teknologi MARA in 2012. She received her Ph.D. degree from the Faculty of Electrical Engineering, UiTM Shah Alam by a fast track program in 2018. Her research interests include radar technology, network sensor, signal processing, and optic fiber laser. She can be contacted at email: nornajwaismail88@gmail.com.

Idnin Pasya Ibrahim is a Senior Lecturer in Department of Computer Science and Engineering, Division of Computer Engineering, University of Aizu, Aizuwakamatsu. He received the Bachelor of Engineering, Master and Ph.D. of Engineering in Information and Communication Engineering from Tokyo Denki. He can be contacted at email: idnin@u-aizu.ac.jp.

Siti Amalina Enche Ab Rahim received the Diplôme d'Ingénieur in electronics and communications engineering from Ecole National Superieur d'Electronique et de Radioelectricite de Grenoble (ENSERG), France in 2008 and received her D.Eng in electrical and electronics engineering from Kyushu University, Japan in 2017. In 2009, she joined Telekom Research and Development Sdn. Bhd (TMRND), Cyberjaya, Malaysia as a researcher, before joining Universiti Teknologi Mara, (UiTM), Shah Alam, Malaysia as a lecturer in 2017. Her current research interests include the design of RF passive components and RF CMOS integrated circuits. She can be contacted at email: amalinaabr@uitm.edu.my.

Nor Ayu Zalina Zakaria is currently a Senior Lecturer at the School of Electrical Engineering, College of Engineering, Universiti Teknologi MARA, Malaysia. In 2017, she received her Ph.D. in Radar Technology from the University of Birmingham, UK and Master in Mobile and Satellite Communication Engineering from University of Surrey, UK in 2003. She completed her BEng (Hons) in Electronics and Telecommunication Engineering from University Malaysia Sarawak in 2000. She can be contacted at email: norayu713@uitm.edu.my.